

Encoding Sensory and Motor Patterns as Time-Invariant Trajectories in Recurrent Neural Networks

Vishwa Goudar² and Dean V. Buonomano^{1,2,3}

¹Integrative Center for Learning & Memory

²Department of Neurobiology

³Department of Psychology

UCLA, Los Angeles, CA, 90095, USA.

Contact: dbuono@ucla.edu

arXiv preprint, January 3, 2017

Abstract:

Much of the information the brain processes and stores is temporal in nature—a spoken word or a handwritten signature is defined as much by how it unfolds in time as by its spatial structure at any given moment in time. It remains unclear how neural circuits encode such patterns. We show that the same recurrent neural network model can simultaneously encode time-varying sensory and motor patterns as *continuous* neural trajectories. Tuning the recurrent weights of the network improves its ability to store target spatiotemporal patterns, by sculpting its dynamics and binding each target pattern to a distinct voyage through neural phase space. Crucially, this representation endows the network with the brain-like property of temporal invariance—the network is able to identify the same stimulus played at different speeds. We demonstrate this framework with a network capable of robustly transcribing spoken digits to “handwritten” digits.

Introduction:

Many, if not most, of the tasks the brain performs are inherently temporal in nature: from recognizing and generating complex spatiotemporal patterns, such as speech and music, to creating temporal expectations of when an event will occur¹⁻⁵. How does the brain encode these complex temporal patterns? One highly influential theory in neuroscience holds that memories are stored as fixed-point attractors that emerge in the dynamic activity of the brain's recurrently connected circuits⁶⁻⁹. Two limitations of this framework are: 1) it fails to capture the temporal aspect of stored information, thus forcing many computational models to "spatialize" time—that is, they treat the temporal component of time-varying patterns as additional spatial dimensions¹⁰⁻¹⁴; 2) it does not capture a fundamental feature of how the brain processes temporal information: temporal invariance. For example, humans readily recognize temporally warped—compressed or dilated—speech or music.

While the mechanisms that underlie the brain's ability to perform a broad range of spatiotemporal tasks in the sensory and motor domains are not known, there is mounting theoretical and experimental evidence that our ability to tell time on the subsecond scale, and represent time-varying patterns, relies on the inherent *continuous* dynamics, and computational potential, of recurrent neural networks¹⁵⁻²⁰. Indeed, recent computational studies have established that by tuning the weights within recurrent neural network (RNN) models, it is possible to robustly store and generate complex time-varying motor patterns²¹⁻²³. What is not known is whether the same approach can be used to robustly discriminate and store time-varying sensory patterns in a manner that allows for the recognition of novel exemplars of learned prototypes. For this to happen, the dynamics of a network must be sensitive to the spatiotemporal structure of the sensory patterns, but largely invariant to the time-varying structured noise of the different exemplars of the same stimuli, as well as to temporal compression and dilation of these stimuli. While earlier studies have demonstrated that training can stabilize the encoding of autonomous neural trajectories that represent motor patterns²¹⁻²³, robust neural encoding of sensory patterns demands invariance to sensory *signal-dependent* noise.

Neuroscientists have typically distinguished between sensory and motor areas; but it is well established that activity in sensory areas is strongly influenced by motor behavior, and that sensory stimuli can modulate activity in motor areas—furthermore, some brain areas are characterized as being sensorimotor²⁴⁻²⁸. Computationally, sensory and motor processing are understood to have disparate requirements—during sensory processing, network dynamics should primarily be driven by the sensory inputs; in contrast, during motor processing neural dynamics should be autonomous and driven primarily by recurrent interactions. It is unclear how a single network could accomplish both tasks, and indeed, to date, no previous models have shown that the same network can satisfy the requirements for both sensory and motor

processing. Here we show that the same RNN can function in both a sensory and motor regime. Specifically the same RNN can convert complex time-varying sensory patterns into motor patterns—thus performing a transcription task in which spoken digits are identified and read out as "handwritten" digits.

In the temporal domain, understanding how the brain recognizes temporally compressed or dilated patterns represents a long-standing challenge. This temporal invariance is particularly evident in our ability to recognize temporally warped speech or music^{29,30}. Our results suggest that one advantage of storing time-varying patterns as neural trajectories within RNNs is that, under the appropriate conditions, this strategy naturally accounts for temporal invariance.

Results:

We first asked if a single RNN could perform a complex sensory-motor task: transcribing spoken digits into handwritten digits. A *continuous-time* firing-rate RNN with randomly assigned recurrent connections was used³¹. The strengths of these recurrent connections were initialized to be relatively strong; thus, before training the network was in a so-called high-gain regime ($g = 1.6$) that is characterized by self-perpetuating and chaotic activity (Experimental Procedures). The transcription task is divided into a sensory and a motor epoch. During the sensory epoch, the RNN is presented with a spoken digit, and over the ensuing motor epoch the RNN drives an output pattern transcribing the presented digit via three motor outputs x , y , and z —activity in the x and y units determines the 2D coordinates of a “pen on paper”, while z determines if the “pen” is in contact with the “paper” or not. **Figure 1A** illustrates the network architecture and transcription task for the digit “2”. Successful performance of this transcription task requires that the RNN: 1) encode spoken digits with a set of neural trajectories in high-dimensional phase space; 2) autonomously generate digit-specific high-dimensional trajectories during the motor epoch, in order to drive the digit-specific output patterns; and most importantly 3) generate trajectories that are stable so they may encode each digit’s sensory pattern, sensory-motor transition, and motor pattern in a manner that is invariant not just to background noise but also to spatiotemporal variations of the spoken digits, including temporal warping.

We attempted to satisfy these three conditions by training the RNN using a supervised learning rule, in which the recurrent units were trained to robustly reproduce their “innate” patterns of activity²¹—that is, those generated in the untrained network—using the recursive-least-squares learning rule^{32,33}. In essence, the RNN is trained to reproduce one digit-specific “innate” trajectory in response to all training utterances of a given digit. For example, the pattern of activity produced in response to a “template” utterance of a given digit from the beginning of the sensory epoch to the end of the motor epoch is taken as the innate trajectory; the network is then trained to reproduce this trajectory in response to other utterances of the same digit. Furthermore, it is trained to do so regardless of the initial state of the network’s units, and in the presence of continuous background noise (Experimental Procedures). Only after training the RNN (*recurrent training*), are the output units trained to generate the handwriting patterns representing each of the digits during the motor epoch—this output training phase is performed using standard supervised methods (Experimental Procedures). **Figure 1B** shows the outputs of a trained network cross-tested on ten digits (0-9) across five speakers. Following training, the network successfully transcribes the utterances used during training (marked by asterisks). More importantly, performance generalizes to novel utterances and speakers in the dataset despite significant variations in the duration and spatiotemporal structure across utterances (**Supplementary Movie 1**).

To quantify performance, we need an objective measure of the quality of the motor output for each test utterance. This itself represents a classification task, wherein images of RNN-generated transcriptions must be assigned to one of the ten possible digits. Rather than use a human-based performance measure, we used a standard deep convolutional neural network (CNN)³⁴ to rate the performance of trained RNNs (Experimental Procedures)—i.e., the CNN was used to determine if each “handwritten” digit was correct or not. Performance of trained RNNs was 98.7% on a test set of 410 novel stimuli (**Fig. 1C**). Since untrained RNNs (“reservoir networks”) are in and of themselves capable of performing many interesting computations³⁵⁻³⁷, it is important to determine how much of this performance is dependent on the training of the RNNs. We thus examined a control group wherein the three output units are trained as they were for the trained RNNs, but the RNN itself was not trained (the “reservoir”). The performance was very poor (20%), in large part because during the motor epoch a reservoir RNN is operating in an autonomous mode that is chaotic—making it difficult for the output units to learn to produce the target output patterns. We also examined the effects of training an RNN only during the motor epoch, resulting in a performance of 71%. This significant improvement over the reservoir networks is a consequence of the fact that a network driven by external inputs can encode sensory stimuli despite a lack of sensory epoch training, due to the stabilizing influence of the external inputs (see below). Yet, despite the improvement in performance, some digits were almost always misclassified (**Supplementary Fig. 1**). The difference in performance between the trained RNNs (sensory and motor training) and the exclusively motor trained RNNs, confirms the importance of tuning the recurrent weights to the sensory discrimination component of the task (see below).

Stability of the Neural Trajectories.

RNNs operating in high-gain regimes are prone to chaotic behavior^{38,39}, because the strong recurrent feedback characteristics of these networks rapidly amplifies any noise or perturbations. It is thus critical to demonstrate that the above performance is robust to background noise and perturbations during the sensory and motor epochs. The distinction between epochs is critical since the RNN is operating in fundamentally different regimes during the sensory and motor epochs. During the sensory epoch the recurrently generated internal dynamics are partially suppressed (or “clamped”) as a result of the external input, yet during the motor epoch all activity is internally generated. To examine the stability of these sensory and motor “object” representations, we briefly perturbed the internal dynamics of the RNN during either the sensory or motor epochs. Sensory epoch perturbations were introduced half way through the presentation of each utterance, while motor epoch perturbations were introduced at the 10% mark of the motor epoch. **Figure 2A** shows the activity of a hundred units from a trained RNN (and the resulting output), when it is presented with the digit “three” and strongly perturbed (amplitude = 2) in the motor epoch. The resulting transcription briefly

deviates from an unperturbed one (grey backdrop), but recovers mid-voyage. The sensory epoch is less sensitive to perturbations—as would be expected because the presence of the external input serves as a stabilizing influence³⁹. During the motor epoch the RNN is operating autonomously as a "dynamic attractor", that is, once bumped off its trajectory it maintains a memory of its current voyage and is able to return to the original trajectory²¹ (**Fig. 2B**). Performance measurements using the CNN classifier reveal a graceful degradation across a wide range of perturbation magnitudes, and confirm the superior robustness of the sensory epoch (**Fig. 2C**).

RNN Training Sculpts Network Dynamics to Enhance Discrimination.

How does tuning the recurrent weights allow the RNN to stably encode both sensory and motor information in neural trajectories, despite considerable spatiotemporal differences between digit utterances (**Fig. 1B**, insets)? Firing rate traces of sample units in a trained RNN show more similar patterns of activity in response to different utterances of the same digit, when compared to a reservoir RNN (**Fig. 3A-B**). To better examine the structure of the population representations, we can visualize and compare the neural trajectories in response to multiple utterances (learned and novel) of the same digit, during the sensory and motor epochs, in principal component analysis (PCA) subspace. The trajectories produced in the untrained network by utterances of the digits "six" and "eight", during the sensory epoch, occupied a fairly large abutting volume of PCA subspace (**Fig. 3C**); and during the motor epoch the trajectories were highly variable—the network strongly and perpetually amplifies the differences between utterances, because it is in a chaotic regime. In contrast, in the trained RNN, sensory epoch trajectories of each digit were restricted to a narrower volume, and better separated from the volume representing the other digit (**Fig. 3D**). During the motor epoch, the trajectories for different utterances of the same digit were constrained to a much narrower tube—reflecting the dynamic attractor—and better separated from the motor trajectories of the other digit. The set of all within-digit trajectories can be thought of as populating a hypertube that delimits the volume of phase space traversed by the digit. During the sensory epoch, this hypertube of trajectories represents a memory of a family of related spatiotemporal objects: the spoken digit. During the motor epoch the network is autonomous, and the hypertube of all within-digit trajectories narrows to a dynamic attractor that represents the “motor memory” of the corresponding handwritten digit.

It is well established that cortical circuits undergo experience-dependent plasticity—a process that seems to result in the optimization or specialization of those circuits to the tasks the animal is exposed to⁴⁰⁻⁴³. The above results (**Fig. 1**) establish that training the RNN does improve discrimination performance—the recurrent weights are tuned to the task at hand—but leaves open the question of how exactly this is accomplished. To answer this question we

asked if the Euclidean distances between trajectories in response to different utterances of the same digit (within-digit distance), and utterances of different digits (between-digit distance), were significantly altered in comparison to the reservoir RNN. As alluded to earlier, training significantly decreases the mean within-digit distances during the sensory epoch (**Fig. 4A**). Importantly, in doing so, it does not diminish the large separations between trajectories of different digits. The same effect, much enhanced, is observed during the motor epoch, a consequence of the formation of dynamic attractors. Successful formation of these attractors is strongly influenced by an unambiguous and stable sensory epoch-motor epoch transition of the network dynamics. This transition relies on the high between-digit separation and low within-digit separation of sensory epoch trajectories, particularly at the end of the sensory epoch—more convergent within-digit sensory encodings result in more stereotyped initial conditions for the motor trajectories, in turn, resulting in the reliable formation of and transition to motor pattern-encoding dynamic attractors.

The finding that training sculpts the dynamics of the RNN during the sensory epoch is also a critical one because it shows that even though RNN activity is governed in part by the external input, the internal connections are critical in that tuning them effectively improves the interaction between the sensory input and the internally generated dynamics. This improvement is expressed as a collapsing of the family of trajectories representing a digit into a narrower hypertube. These results follow as a direct consequence of the supervised recurrent training paradigm (Experimental Procedures)—a single innate trajectory serves as a common target for different training utterances of a digit, thereby inducing changes in the network’s recurrent dynamics that are necessary to encode the different utterances along similar neural trajectories; However, different digits are encoded in rapidly divergent trajectories because the target trajectories for each digit are generated by an untrained chaotic network. Further evidence that training dramatically influences the weight matrix of the RNN is demonstrated by the change in its eigenspectrum (**Fig. 4B**). Because the network is initialized with normally distributed weights with a gain of 1.6 (Experimental Procedures), the eigenspectrum of the reservoir’s weight matrix lies in a circle of radius approximately 1.6. Training results in a compression of those eigenvalues with real part larger than one, bringing the maximal real part of the eigenvalues closer to one. In a linear network, when all eigenvalues have a real part less than one, it implies that the network’s activity will decay to zero when it operates autonomously; however our network is nonlinear and does not operate exclusively in the autonomous mode, so interpretations of the eigenspectrum of the weight matrix are not straightforward—nevertheless the compression of the eigenspectrum is consistent with the increased stability of the network during the sensory and motor epochs^{44,45}.

To better characterize how the plasticity of the recurrent weights shapes the dynamics and computational effectiveness of the RNN, we developed a novel analysis based on the decomposition of the RNN drive into its input and recurrent components. The results of this

decomposition analysis show that training results in the recurrent weights suppressing deviations between within-digit neural trajectories, thereby driving them closer together (**Supplementary Figs. 2, 3**). Training with a common within-digit target trajectory exposes the spatiotemporal distribution of the within-digit variations in the sensory input—it separates the sensory input “signal” from this signal-dependent “noise”—and in doing so, allows for effective sampling from this distribution. Training then shapes the basins of attraction around the spoken digit-encoding trajectories based on this distribution, resulting in effective, recurrently-driven suppression of the input noise.

Balance between Internal and Input Dynamics is Crucial for Discrimination.

The above results provide insights as to how a single neural circuit can function in two seemingly distinct computational modes: sensory and motor. Sensory discrimination requires circuits to be highly responsive to external stimuli in order to categorize inputs into discrete classes. In contrast, motor tasks require autonomous generation of spatiotemporal patterns, and thus need the network dynamics to be somewhat resistant to external inputs. In the network described here, this balance depends on the recurrent weights and the magnitude of the external drive.

The recurrent weights must be strong—that is the network must be in a high-gain regime—for two reasons. First, network dynamics in high-gain regimes are high-dimensional⁴⁶, which naturally yields well-separated trajectories for different digits. A goal of training then, is to achieve recurrent suppression of within-digit separation, while retaining the large between-digit separation (**Fig. 4, Supplementary Fig. 3**). Second, as noted earlier, a network operating in a high-gain regime is inherently capable of generating the self-perpetuating activity required in the motor epoch, which is then stabilized by the training procedure. Thus during the sensory epoch, the RNN is operating in a regime that is both sensitive to external input and influenced by strong internal recurrent dynamics. In the motor mode, the RNN operates autonomously, generating locally stable trajectories that serve as a high-dimensional “engine” that drives arbitrary low dimensional output patterns.

The ability of the network to meaningfully process input patterns during the sensory epoch, so that they are easy to discriminate, also depends on the strength of the inputs. To better understand the impact of input amplitude on the encoding trajectories and their discriminability, before and after training, we parametrically varied the input amplitude and studied the resulting RNN dynamics during the sensory epoch. In the reservoir, both within and between-digit distances diminish as the input amplitude increases (**Fig. 5A, left panel**), consistent with a previous study showing that strong inputs can progressively dominate and override the internal dynamics of an RNN³⁹. In the extreme, input-dominated regimes effectively void the recurrent

weights and render training useless (**Fig. 5A, right panel**). The poor discriminability at high input amplitudes is further confirmed by dimensionality measurements of sensory epoch trajectories (Experimental Procedures), which mirror the low-dimensionality of the input cochleograms, regardless of training (**Fig. 5B**). In contrast, low-input amplitude regimes are dominated by the RNN’s internal dynamics. Reservoirs in this regime produce chaotic high-dimensional dynamics and are insufficiently sensitive to external inputs; thus the within- and between-digit distances are similarly high (**Fig. 5A, left**). Training strongly alters these dynamics, lowering its dimensionality (**Fig. 5B**). However, as a consequence of poor input-sensitivity, these changes fail to improve discrimination—trained RNNs in this regime still sustain similar within and between-digit distances (**Fig. 5B, right**). RNNs trained at intermediate input amplitudes (0.5, 5) are both sensitive to the input and able to discriminate between digits, because their sensory epoch trajectories are shaped both by the input and internal dynamics. It is thus critical that the input drive be strong enough to influence ongoing activity but not strong enough to "erase" recent information encoded in the current trajectory.

Continuous Trajectories are Invariant to Temporal Warping.

As mentioned above, a signature and little understood feature of how the brain processes time-varying patterns pertains to temporal warping (temporal invariance), whereby temporally compressed or dilated input signals can be identified as the same pattern. Thus an important test for computational models of sensory processing of time-varying stimuli, is whether they are able to account for temporal invariance. We hypothesized that one advantage of encoding time-varying stimuli as continuous neural trajectories, is that it naturally addresses the problem of temporal warping; specifically, that compressed or dilated stimuli generate similar neural trajectories that play out at different "speeds"^{47,48}. To test this hypothesis we trained and tested an RNN on a dataset of temporally warped spoken digits. Specifically, the input pattern, $\mathbf{y}(t)$, of a single utterance of each digit from a speaker of the TI-46 dataset was artificially stretched or compressed by a time warp factor α ($\mathbf{y}(\alpha t)$), while retaining its spectral structure. **Figure 6A** (left panel) shows the input structure for two utterances of the digit “nine”, one warped to twice and the other to half the duration of the original utterance.

The RNN was trained on three utterances of each digit (warp factors of 0.7, 1 and 1.4) and tested on warp factors in the range 0.5 to 2 (a four-fold factor that approximates the natural speed variation of speech). To discern the effect of a temporally warped input on the encoding trajectory, we constructed a matrix of the distances between trajectories produced by the reference ($\alpha=1$) and a warped utterance (**Fig. 6A**). Each element of such a matrix measures the distance between the two trajectories at a corresponding pair of time points. In the case of perfect warping (e.g., when the reference trajectory and the trajectory at an $\alpha \neq 1$ overlap exactly in phase space), a straight diagonal line of zero distances (deep blue) would be

observed during the sensory epoch (shaded region), with slope proportional to the warp factor. Trajectories produced by temporally warped inputs in the sensorimotor trained RNN were closer to the reference compared to their counterparts in the reservoir or motor-trained RNN. In other words tuning the recurrent weights dramatically improved the ability of the network to reproduce the same neural trajectories, despite being driven by inputs at different speeds. We quantified this effect by measuring the average distance between the reference and warped trajectories during the sensory epoch over different warp factors (**Fig. 6B**). In comparison to the two control networks, the trained RNN maintains a much smaller distance between trajectories across the four-fold range of temporal warping—including warp factors outside the range used during training. These results confirm the hypothesis that training produces an interaction between the internal dynamics and external input that renders the encoding trajectories invariant to temporal warping of the input patterns. The impact of this result is borne out in the network's performance on the digit transcription task, as measured by the CNN classifier (**Fig. 6C**). Training during the sensory and motor epochs dramatically improves "extrapolation"—that is generalization to speeds outside the range of training speeds; however, training during the motor epoch alone is sufficient to produce very good "interpolation" (novel speeds within the training set range) generalization. This confirms the hypothesis that an inherent computational advantage of encoding time-varying sensory stimuli in neural trajectories is that it naturally addresses the temporal invariance problem.

Discussion:

The brain naturally encodes, recognizes, and generates complex time-varying patterns, and can seamlessly process temporally warped patterns. Despite our poor understanding of these processes, theoretical evidence increasingly suggests that the dynamics of recurrently connected circuits in the brain are critical to representing time-varying patterns. For example, so-called reservoir computing approaches propose that complex high-dimensional spatiotemporal patterns are represented in the dynamics inherent to randomly connected recurrent neural networks^{16,33,35}. A shortcoming of this approach, however, is that the recurrent connections in these networks are not plastic; thus in contrast to actual cortical circuits, the random recurrent neural network (the "reservoir") does not adapt or optimize to the task at hand. Additionally, fully tapping into the computational potential of randomly connected RNNs has proven difficult because they are susceptible to chaos^{38,49}. However, progress has been made on both accounts^{21,50,51}. Here, we extend these results to better understand well-known aspects of the brain's ability to represent time-varying sensory *and* motor patterns—we demonstrate how experience-dependent plasticity could reshape the dynamics of reservoir RNNs to qualitatively improve representations by endowing them with such essential properties as generalization to novel exemplars, sensor-motor association and transformation, and temporal invariance.

An earlier study enlisted synaptic conductance-based dynamics to achieve temporal warping⁵²; In contrast, the model described here illustrates that encoding temporal patterns within the neural trajectories of recurrent networks naturally enables dynamic pattern recognition of time-warped stimuli. Specifically, one advantage of encoding dynamic patterns as neural trajectories is that the trajectories themselves are in a sense "time-independent entities" (e.g., phase space is "timeless"). In practice, however, RNNs in high-gain regimes are highly sensitive to any change in the driving input, including to the input speed (as shown by the performance of the reservoir network). Yet, by training the RNN, it is possible to reshape its dynamics such that temporally warped sensory stimuli are encoded by more or less similar trajectories in neural phase space.

Our results also demonstrate how training an RNN reveals a computationally powerful input processing regime, one that helps generalize the encoding of learned time-varying patterns to novel exemplars. As stated earlier, recognizing different instances of the same digit as one and the same, while discriminating between different digits requires that networks actively and differentially sculpt the within and between class trajectories—the separation between trajectories representing similar patterns must be kept to a minimum, while that between trajectories representing different patterns must be amplified. A previous study has analytically shown that untrained random recurrent networks (reservoir networks) process inputs in one of three computational regimes: a chaotic regime, wherein any separation between trajectories is

strongly amplified by the network's chaotic dynamics; a regime with weak recurrent weights that is input-dominated with little computational power; and a critical regime wherein the input and internal dynamics are balanced⁵³. Here, we show that training alters these regimes in very different ways (**Fig. 5**). Crucially, relative to the separation between the input patterns, reservoir networks in the critical regime amplify the separation between trajectories representing similar patterns more strongly than between different patterns Fig. 4 in ⁵³. In contrast, trained networks separate trajectories according to the patterns they are representing (**Fig. 5A**). Tuning the recurrent weights reshapes the internal dynamics of the network, resulting in a recurrent component that redirects or suppresses deviations from the target trajectories (**Supplementary Figs. 2-3**). Ultimately, it is this property of trained networks that allows them to encode complex sensory patterns and effectively generalize across utterances and speakers.

The computational potential of continuous time RNNs in high-gain regimes has long been recognized, but it has been challenging to tap into this potential because of their inherently chaotic behavior and the difficulties in training them^{54,55}. Step-by-step, progress has been made on how to capture the computational potential of RNNs^{21,33,35,50}. Here we establish that a further feature of trained RNNs is their ability to not only encode spatiotemporal objects, but to perform complex sensorimotor tasks and address the long-standing problem of temporal warping. We propose that spatiotemporal objects are not encoded as fixed-point attractors, but as locally stable neural trajectories. An experimentally tractable prediction that emerges is that neural trajectories will be stable in response to local perturbations—potentially administered through optogenetic stimulation—and that the neural trajectories elicited during sensory stimuli will be more resistant to perturbations than the neural trajectories unfolding during the motor epoch of sensory-motor tasks. Finally, our results also predict that compared to sensory and motor areas, the relative and absolute strength of input and recurrent synapses will be different in sensorimotor areas. Specifically, their recurrent weights will be stronger than in sensory areas, and input weights will be stronger than in the motor areas.

Methods:

Network Model

The dynamics of the RNN was comprised of N nonlinear continuous-time firing rate units modeled as:

$$\tau \frac{dx_i}{dt} = -x_i + \sum_{j=1}^N W_{ij}^R r_j + \sum_{j=1}^M W_{ij}^I y_j + I_i^{noise} \quad (1)$$

$$r_i = \tanh(x_i) \quad (2)$$

x_i represents the state of neuron i , and r_i its “firing rate”. The time constant, τ , of each unit was set to 25 ms. \mathbf{W}^R is the weight matrix representing the recurrent connectivity of the network. The recurrent connectivity was uniformly random (but with no autapses) with a connection probability (p_c) of 0.2. The weights of these synapses were initialized from an independent Gaussian distribution with zero mean and SD equal to $g/\sqrt{p_c N}$, where g represents the “gain” of the network. RNNs were initialized to a high-gain regime ($g = 1.6$), which generates chaotic self-perpetuating activity in the absence of external input or noise³⁸.

The M -dimensional vector $\mathbf{y}(t)$ represents the time-varying external input to the RNN. The fixed input weight matrix, \mathbf{W}^I , tonotopically projects this input vector onto the RNN—input channel k is projected onto units $(k-1) \times N/M + 1$ thru $k \times N/M$. The weights of these connections were drawn from an independent Gaussian distribution with zero mean and unit variance. The handwriting was modeled with 3 output units (o_1, o_2, o_3) that represented the x, y and z coordinates of a pen on paper. Finally, each unit of the RNN also received an independent noise current, I_i^{noise} , modeled as additive Gaussian white noise with SD I_0 .

As is standard, the output neurons were simulated as a weighted linear sum of all the units in the RNN:

$$o_i = \sum_{j=1}^N W_{ij}^O r_j \quad (3)$$

where the output weight matrix, \mathbf{W}^O , was initialized from an independent Gaussian distribution with zero mean and SD $1/\sqrt{N}$. All simulations were performed with a time step of 1 ms.

Simulations and Training

Each trial consisted of a time window comprised of a sensory and a motor epoch. We defined the sensory epoch as the period in which an external stimulus is presented—starting at $t=0$ and lasting the duration of the utterance. The motor epoch was defined as a period beginning 300 ms after the sensory epoch ended and lasting the duration of the target motor pattern (the appropriate handwritten digit).

Training proceeded in three steps (described in detail below): (1) target trajectories were generated for each utterance of each digit in the training subset of the dataset; (2) the recurrent units were trained to reproduce the target trajectories; and (3) the output units were

trained to produce the handwritten spatiotemporal patterns. The trained network was then tested on novel (and trained) utterances. In steps 2, 3 and during testing, each trial began at $t=-100$ ms with the network initialized to a random state (x_i values drawn from a uniform distribution between -1 and 1). In **Figs. 1, 6** and **Supplementary Fig. 1**, testing was performed with the noise amplitude (I_0) set to 0.05. For the perturbation analysis (**Fig. 2**), a 25 ms “perturbation pulse” was introduced during the sensory or motor epoch of each trial, with I_0 set to the desired perturbation magnitude for the duration of the pulse. Noise was omitted in these simulations to allow for a direct assessment of the effects of the perturbation pulse. Similarly, for the simulations in **Figs. 3-5** and **Supplementary Fig. 3**, noise was omitted ($I_0=0$) so that the impact of training on the generalization and discriminability of an RNNs encodings, but not its noise invariance, could be direct evaluated.

Simulations of the untrained “reservoir” control network skipped steps 1 and 2, while simulations of the motor-trained control network limited recurrent network training (step 2) to a duration starting 150 ms after the end of the sensory epoch and lasting until the end of the motor epoch.

Input Structure

We used spoken digits from the TI-46 spoken word corpus⁵⁶ to train and test networks on the transcription task. Specifically, our dataset was composed of the spoken digits “zero” thru “nine”, uttered 10 times each, by each of five female subjects. Spoken digits from the corpus were decoded, end-pointed, resampled to 12 kHz, and converted to spectrograms with Matlab’s specgram function. The spectrograms were preprocessed with Lyon’s passive ear model of the human cochlea⁵⁷, as implemented by the auditory toolbox (Malcolm Slaney), to generate analog “cochleograms” composed of 12 analog frequency bands, or channels, ranging from 0 to 6 kHz. Finally, the cochleograms were smoothed with a 20th order 1D median filter (Matlab’s medfilt1 function), normalized to a maximum of 1 (i.e., they were normalized by the maximal value of all utterances and digits), and scaled by an input amplitude. During the sensory epoch of each trial, the input, $\mathbf{y}(t)$ ($M=12$), took values from the cochleogram corresponding to the utterance that was to be presented to the RNN. At all other times of the trial, $\mathbf{y}(t)$ was set to 0. The input amplitude was set to 5 in all simulations except in **Fig. 5**, where it was parametrically varied. For the temporal warping simulations (**Fig. 6**) the cochleograms were compressed or dilated by the warping factor α through linear interpolation.

Innate Trajectories and RNN Training

Training was performed with the “innate-learning” approach—which uses the Recursive Least Squares (RLS) rule to train each unit of the recurrent network to match the pattern generated by the untrained network²¹. For each subject used in the training set, a single template utterance of each digit was presented to the untrained RNN (the reservoir) in the absence of background noise, and the resulting trajectory served as a target (“innate”) trajectory. The template utterance of each digit was chosen as one with the median duration among all the utterances of the digit by the subject. Target sensory epoch trajectories for other training utterances of the digit by the same subject were generated by linearly warping this innate trajectory to match the utterance durations.

The initial network state was chosen at random while harvesting the target trajectory for each digit. Target trajectories for template utterances of the same digit by different speakers were harvested starting the network at the same initial state. To achieve the formation of digit-specific dynamic attractors, the same target motor trajectories were used for all utterances of each digit. All networks were trained with three utterances of each digit for each of the subjects in the training set. The networks in **Fig. 1** and **Supplementary Fig. 1** were trained on three subjects and tested on five, while those in **Figs. 2-6** and **Supplementary Fig. 3** were trained and tested on 1 subject.

Network training was performed by modifying the recurrent weight matrix, \mathbf{W}^R , with the Recursive Least Squares learning rule³². The rule was simultaneously applied to 90% of the units in the network (randomly selected). Training was conducted by iterating through all utterances of the digits in the training set over multiple trials, starting each trial at a random initial condition and continuously injecting the network with background noise (I^{noise}). Training concluded when the error in the activity of the rate units asymptoted (generally between 100 and 150 trials).

Output Training

The spatiotemporal target patterns that comprise the handwritten digits were sampled from a Wacom Bamboo Pen Tablet, as the digits “0” thru “9” were individually stenciled on it. For each handwritten digit, the x and y coordinates of the pen were sampled at approximately 50 Hz, low-pass filtered, and resampled with interpolation to 1 kHz (corresponding to the 1 ms simulation time step). The target values for o_1 and o_2 were set to 0 from the start of each trial until the beginning of the motor epoch. During the motor epoch, they were set to the pen’s 2D coordinates for the corresponding digit, and reset to 0 between the end of the motor epoch and the end of the trial. The target for o_3 (z co-ordinate) was a step function, set to 1 during the motor epoch and 0 at all other times. To train the output units, the Recursive Least Squares learning rule was applied to the readout weights in \mathbf{W}^O ^{21,32,33,35}. Output training was performed for 25 trials per utterance of each digit in the training set, while the RNN was continuously injected with background noise.

In each test trial, the motor output was recorded from the values of o_1 and o_2 , whenever the value of o_3 was greater than 0.5 (i.e. when “the pen contacted the paper”). At the end of the trial, a 28×28 pixel grayscale image of the “handwritten” output (pen width = 2 pixels) was labeled as the transcription for the corresponding digit. An objective determination of the transcription’s accuracy was made by comparing this label to one assigned to the image by a CNN classifier for handwritten digits. This classification was performed with the LeNet-5 CNN classifier⁵⁸ implemented with the Caffe deep learning framework⁵⁹. The CNN was first trained on the MNIST database of handwritten digits⁶⁰, and its output layer was then fine-tuned on the stenciled digits that we used as the output targets.

Trajectory Analysis

For **Fig. 3**, Principal Component Analysis (PCA) was performed on a concatenation of the trajectories generated by both the reservoir and the trained network in response to all utterances of the digits “six” and “eight” by a single subject. Trajectories were then individually projected onto three principal components and plotted in 3D. The sensory (motor) trajectories

were projected onto PCs 2-4 (PCs 1-3). PC 1 was not used in plotting the sensory trajectories, because it captured features common to both spoken digits.

In **Figs. 4, 5**, the sensory (motor) epoch within-digit distances were calculated from the Euclidean distance, at each time step, between the sensory (motor) epoch trajectory for each utterance, and its nearest neighbor from among the sensory (motor) epoch trajectories encoding training utterances of the same digit (except itself). Similarly, the sensory (motor) epoch between-digit distances were calculated from the Euclidean distance, at each time step, between the sensory (motor) epoch trajectory for each utterance, and its nearest neighbor from among the sensory (motor) epoch trajectories encoding training utterances of all other digits. Trajectory distances in **Fig. 6B** were calculated in a similar fashion: at each time step, the Euclidean distance was calculated between the trajectory encoding an utterance at warp factor α ($I_0=0.05$), and its nearest neighbor along the trajectory encoding the reference utterance of the same digit ($I_0=0$). The time-average of these distances were then summarized over 10 trials for the plot in **Fig. 6B**. Finally in **Supplementary Fig. 3**, sensory epoch within-digit distances were calculated from the minimum distance, at each time step, of the sensory epoch trajectory for each novel utterance of each digit from the sensory epoch trajectory for each trained utterance of the same digit. We refer to this procedure of aligning trajectories based on their minimum distance at each time point as temporal alignment.

The dimensionality measure shown in **Fig. 5** was calculated as $\left(\sum_{k=1}^N \lambda_k^2\right)^{-1}$, where λ_k represents eigenvalues of the equal-time cross-correlation matrix of network activity, expressed as a fraction of their sum⁴⁶. The eigenvalues were calculated on a concatenation of the sensory epoch trajectories for all utterances (trained and novel) of all digits.

References:

- 1 Nobre, A. C., Correa, A. & Coull, J. T. The hazards of time. *Current Opinion in Neurobiology* **17**, 465-470, doi:<http://dx.doi.org/10.1016/j.conb.2007.07.006> (2007).
- 2 Ivry, R. B. & Schlerf, J. E. Dedicated and intrinsic models of time perception. *Trends in Cognitive Sciences* **12**, 273-280, doi:10.1016/j.tics.2008.04.002 (2008).
- 3 Mauk, M. D. & Buonomano, D. V. The Neural Basis of Temporal Processing. *Ann. Rev. Neurosci.* **27**, 307-340 (2004).
- 4 Merchant, H., Harrington, D. L. & Meck, W. H. Neural Basis of the Perception and Estimation of Time. *Annual Review of Neuroscience* **36**, 313-336, doi:doi:10.1146/annurev-neuro-062012-170349 (2013).
- 5 Hopfield, J. J. Understanding Emergent Dynamics: Using a Collective Activity Coordinate of a Neural Network to Recognize Time-Varying Patterns. *Neural Computation* **27**, 2011-2038, doi:10.1162/NECO_a_00768 (2015).
- 6 Hopfield, J. J. & Tank, D. W. Computing with neural circuits: a model. *Science* **233**, 625-633 (1986).
- 7 Hopfield, J. J. Neural networks and physical systems with emergent collective computational abilities. *Proc Natl Acad Sci U S A* **79**, 2554-2558 (1982).
- 8 Wang, X. J. Synaptic reverberation underlying mnemonic persistent activity. *Trends Neurosci.* **24**, 455-463 (2001).
- 9 Amit, D. J. & Brunel, N. Model of global spontaneous activity and local structured activity during delay periods in the cerebral cortex. *Cereb Cortex* **7**, 237-252 (1997).
- 10 Elman, J. L. Finding Structure in Time. *Cog. Sci.* **14**, 179-211 (1990).
- 11 Mnih, V. *et al.* Human-level control through deep reinforcement learning. *Nature* **518**, 529-533, doi:10.1038/nature14236 (2015).
- 12 Hinton, G. *et al.* Deep Neural Networks for Acoustic Modeling in Speech Recognition: The Shared Views of Four Research Groups. *Signal Processing Magazine, IEEE* **29**, 82-97, doi:10.1109/MSP.2012.2205597 (2012).
- 13 Rabiner, L. A tutorial on hidden Markov models and selected applications in speech recognition. *Proceedings of the IEEE* **77**, 257-286, doi:10.1109/5.18626 (1989).
- 14 Waibel, A., Hanazawa, T., Hinton, G., Shikano, K. & Lang, K. J. Phoneme recognition using time-delay neural networks. *Acoustics, Speech and Signal Processing, IEEE Transactions on* **37**, 328-339 (1989).
- 15 Rabinovich, M., Huerta, R. & Laurent, G. Transient Dynamics for Neural Processing. *Science* **321**, 48-50, doi:10.1126/science.1155564 (2008).
- 16 Buonomano, D. V. & Maass, W. State-dependent Computations: Spatiotemporal Processing in Cortical Networks. *Nat Rev Neurosci* **10**, 113-125, doi:10.1038/nrn2558 (2009).
- 17 Mante, V., Sussillo, D., Shenoy, K. V. & Newsome, W. T. Context-dependent computation by recurrent dynamics in prefrontal cortex. *Nature* **503**, 78-84, doi:10.1038/nature12742 (2013).
- 18 Carnevale, F., de Lafuente, V., Romo, R., Barak, O. & Parga, N. Dynamic Control of Response Criterion in Premotor Cortex during Perceptual Detection under Temporal Uncertainty. *Neuron* **86**, 1067-1077, doi:<http://dx.doi.org/10.1016/j.neuron.2015.04.014> (2015).
- 19 Crowe, D. A., Zarco, W., Bartolo, R. & Merchant, H. Dynamic Representation of the Temporal and Sequential Structure of Rhythmic Movements in the Primate Medial Premotor Cortex. *The Journal of Neuroscience* **34**, 11972-11983, doi:10.1523/jneurosci.2177-14.2014 (2014).

- 20 Li, N., Daie, K., Svoboda, K. & Druckmann, S. Robust neuronal dynamics in premotor cortex during motor planning. *Nature* **advance online publication**, doi:10.1038/nature17643 (2016).
- 21 Laje, R. & Buonomano, D. V. Robust timing and motor patterns by taming chaos in recurrent neural networks. *Nat Neurosci* **16**, 925-933, doi:10.1038/nn.3405 (2013).
- 22 Rajan, K., Harvey, Christopher D. & Tank, David W. Recurrent Network Models of Sequence Generation and Memory. *Neuron*, doi:10.1016/j.neuron.2016.02.009 (2016).
- 23 Abbott, L. F., DePasquale, B. & Memmesheimer, R.-M. Building functional networks of spiking model neurons. *Nat Neurosci* **19**, 350-355, doi:10.1038/nn.4241 (2016).
- 24 Ayaz, A., Saleem, Aman B., Schölvink, Marieke L. & Carandini, M. Locomotion Controls Spatial Integration in Mouse Visual Cortex. *Current Biology* **23**, 890-894, doi:<http://dx.doi.org/10.1016/j.cub.2013.04.012> (2013).
- 25 Doupe, A. J. & Kuhl, P. K. Birdsong and human speech: common themes and mechanisms. *Annu Rev Neurosci* **22**, 567-631 (1999).
- 26 Schneider, D. M. & Mooney, R. Motor-related signals in the auditory system for listening and learning. *Current Opinion in Neurobiology* **33**, 78-84, doi:<http://dx.doi.org/10.1016/j.conb.2015.03.004> (2015).
- 27 Chang, E. F., Niziolek, C. A., Knight, R. T., Nagarajan, S. S. & Houde, J. F. Human cortical sensorimotor network underlying feedback control of vocal pitch. *Proceedings of the National Academy of Sciences* **110**, 2653-2658 (2013).
- 28 Cheung, C., Hamiton, L. S., Johnson, K. & Chang, E. F. The auditory representation of speech sounds in human motor cortex. *eLife* **5**, e12577, doi:10.7554/eLife.12577 (2016).
- 29 Sebastián-Gallés, N., Dupoux, E., Costa, A. & Mehler, J. Adaptation to time-compressed speech: Phonological determinants. *Perception & Psychophysics* **62**, 834-842, doi:10.3758/bf03206926 (2000).
- 30 Miller, J. L., Grosjean, F. & Lomanto, C. Articulation Rate and Its Variability in Spontaneous Speech - a Reanalysis and Some Implications. *Phonetica* **41**, 215-225 (1984).
- 31 Sompolinsky, H., Crisanti, A. & Sommers, H. J. Chaos in random neural networks. *Physical Rev. Let.* **61**, 259-262 (1988).
- 32 Haykin, S. *Adaptive Filter Theory*. (Prentice Hall, 2002).
- 33 Sussillo, D. & Abbott, L. F. Generating Coherent Patterns of Activity from Chaotic Neural Networks. *Neuron* **63**, 544-557 (2009).
- 34 LeCun, Y., Bengio, Y. & Hinton, G. Deep learning. *Nature* **521**, 436-444 (2015).
- 35 Jaeger, H. & Haas, H. Harnessing nonlinearity: predicting chaotic systems and saving energy in wireless communication. *Science* **304**, 78-80 (2004).
- 36 Maass, W., Natschl, ger, T. & Markram, H. Real-Time Computing Without Stable States: A New Framework for Neural Computation Based on Perturbations. *Neural Computation* **14**, 2531-2560, doi:10.1162/089976602760407955 (2002).
- 37 Lukoševičius, M. & Jaeger, H. Reservoir computing approaches to recurrent neural network training. *Computer Science Review* **3**, 127-149, doi:<http://dx.doi.org/10.1016/j.cosrev.2009.03.005> (2009).
- 38 Sompolinsky, H., Crisanti, A. & Sommers, H. J. Chaos in Random Neural Networks. *Physical Review Letters* **61**, 259-262 (1988).
- 39 Rajan, K., Abbott, L. F. & Sompolinsky, H. Stimulus-dependent suppression of chaos in recurrent neural networks. *Physical Rev. E* **82**, 011903(011905) (2010).
- 40 Buonomano, D. V. & Merzenich, M. M. Cortical plasticity: from synapses to maps. *Annual Rev. Neuroscience* **21**, 149-186 (1998).

- 41 Feldman, D. E. & Brecht, M. Map plasticity in somatosensory cortex. *Science* **310**, 810-815 (2005).
- 42 Karmarkar, U. R. & Dan, Y. Experience-dependent plasticity in adult visual cortex. *Neuron* **52**, 577-585 (2006).
- 43 Crist, R. E., Li, W. & Gilbert, C. D. Learning to see: experience and attention in primary visual cortex. *Nature neuroscience* **4**, 519-525 (2001).
- 44 Ostojic, S. Two types of asynchronous activity in networks of excitatory and inhibitory spiking neurons. *Nature neuroscience* **17**, 594-600 (2014).
- 45 Rajan, K. & Abbott, L. F. Eigenvalue spectra of random matrices for neural networks. *Physical review letters* **97**, 188104 (2006).
- 46 Rajan, K., Abbott, L. & Sompolinsky, H. Inferring Stimulus Selectivity from the Spatial Structure of Neural Network Dynamics. *Advances in Neural Information Processing Systems* **23** (2010).
- 47 Mello, G. B. M., Soares, S. & Paton, J. J. A scalable population code for time in the striatum. *Curr Biol* **9**, 1113-1122 (2015).
- 48 Lerner, Y., Honey, C. J., Katkov, M. & Hasson, U. Temporal scaling of neural responses to compressed and dilated natural speech. *J Neurophysiol* **111**, 2433-2444 (2014).
- 49 Wallace, E., Maei, H. R. & Latham, P. E. Randomly Connected Networks Have Short Temporal Memory. *Neural computation* **25**, 1408-1439 (2013).
- 50 Martens, J. & Sutskever, I. Learning recurrent neural networks with Hessian-free optimization. *Proc. 28th Int. Conf. Machine Learn.* (2011).
- 51 Vogels, T. P., Sprekeler, H., Zenke, F., Clopath, C. & Gerstner, W. Inhibitory Plasticity Balances Excitation and Inhibition in Sensory Pathways and Memory Networks. *Science* **334**, 1569-1573, doi:10.1126/science.1211095 (2011).
- 52 Gütig, R. & Sompolinsky, H. Time-Warp-Invariant Neuronal Processing. *PLoS Biology* **7**, e1000141, doi:10.1371/journal.pbio.1000141 (2009).
- 53 Bertschinger, N. & Natschläger, T. Real-time computation at the edge of chaos in recurrent neural networks. *Neural Comput.* **16**, 1413-1436, doi:10.1162/089976604323057443 (2004).
- 54 Bengio, Y., Simard, P. & Frasconi, P. Learning long-term dependencies with gradient descent is difficult. *IEEE Trans Neural Netw* **5**, 157-166, doi:10.1109/72.279181 (1994).
- 55 Pearlmutter, B. A. Gradient calculation for dynamic recurrent neural networks: A survey. *IEEE Trans. on Neural Network* **6**, 1212-1228 (1995).
- 56 Mark Liberman, R. A., Ken Church, Ed Fox, Carole Hafner, Judy Klavans, Mitch Marcus, Bob Mercer, Jan Pedersen, Paul Roossin, Don Walker, Susan Warwick, Antonio Zampolli. (Linguistic Data Consortium, Philadelphia, 1993).
- 57 Lyon, R. F. in *Acoustics, Speech, and Signal Processing, IEEE International Conference on ICASSP '82*. 1282-1285.
- 58 Lecun, Y., Bottou, L., Bengio, Y. & Haffner, P. Gradient-based learning applied to document recognition. *Proceedings of the IEEE* **86**, 2278-2324, doi:10.1109/5.726791 (1998).
- 59 Jia, Y. *Caffe: An open source convolutional architecture for fast feature embedding*, <<http://caffe.berkeleyvision.org/>> (2013).
- 60 LeCun, Y., Cortes, C. & Burges, C. J. C. *The MNIST database of handwritten digits*, <<http://yann.lecun.com/exdb/mnist/>> (1998).

Acknowledgements:

This research was supported by the NSF (IIS-1420897) and a Google Faculty Research Award. We thank Nicholas Hardy, Omri Barak, Alexandre Rivkind and Jonathan Kadmon for helpful discussions, and Dharshan Kumaran for comments on an earlier version of this manuscript.

Author Contributions:

V.G. and D.V.B. designed the experiments, wrote the code, and wrote the paper.

V.G. performed the simulations and data analysis.

D.V.B. conceived of the approach.

Competing Financial Interests:

None.

Figures:

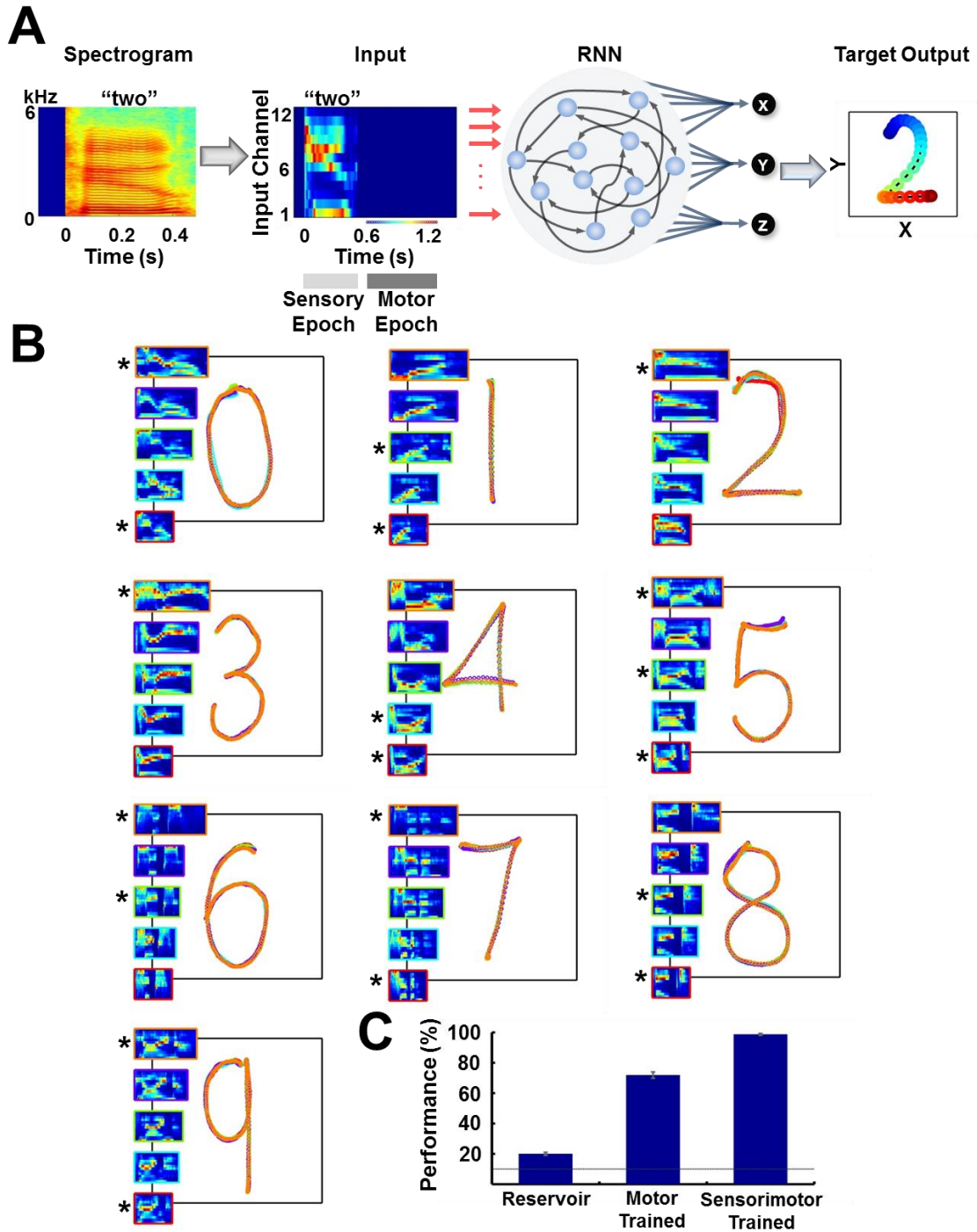


Figure 1: Trained RNNs perform a sensorimotor spoken-to-handwritten digit transcription task.

(A) Transcription task. The spectrogram of a spoken digit, e.g. “two”, is transformed to a 12-channel cochleogram that serves as the continuous-time input to a RNN during the sensory epoch of each trial. During the motor epoch, the output units must transform the high-

dimensional RNN activity into a low-dimensional “handwritten” motor pattern corresponding to the spoken digit (the z output unit indicates whether the pen is in contact with the “paper”). The colors of the output pattern (right panel) represent time (as defined in the “Input” panel). **(B)** Overlaid outputs of a trained RNN ($N=4000$) for 5 sample utterances of each of 10 digits. For all digits, each output pattern is color-coded to the bounding box of the corresponding cochleogram (inset). Sample utterances shown are a mix of trained (*) and novel utterances, and span the range of utterance durations in the dataset. **(C)** Transcription performance of three different types of RNNs on novel utterances. Performance was based on images of the output as classified by a deep CNN handwritten digit classifier. The control groups include untrained RNNs (“reservoir”) and RNNs trained only during the motor epoch (i.e., just to reproduce the handwritten patterns; see Supplementary Fig. 1). Output unit training was performed identically for all networks. Bars represent mean values over 3 replications, and error bars indicate standard errors of the mean. Line indicates chance performance (10%). The RNNs were trained on 90 utterances (10 digits, 3 subjects, 3 utterances per subject per digit). They were then tested on 410 novel utterances (across five speakers, including two novel speakers), with 10 test trials per utterance. I_0 was set to 0.5 during network training (if applicable), and to 0.05 during output training and testing.

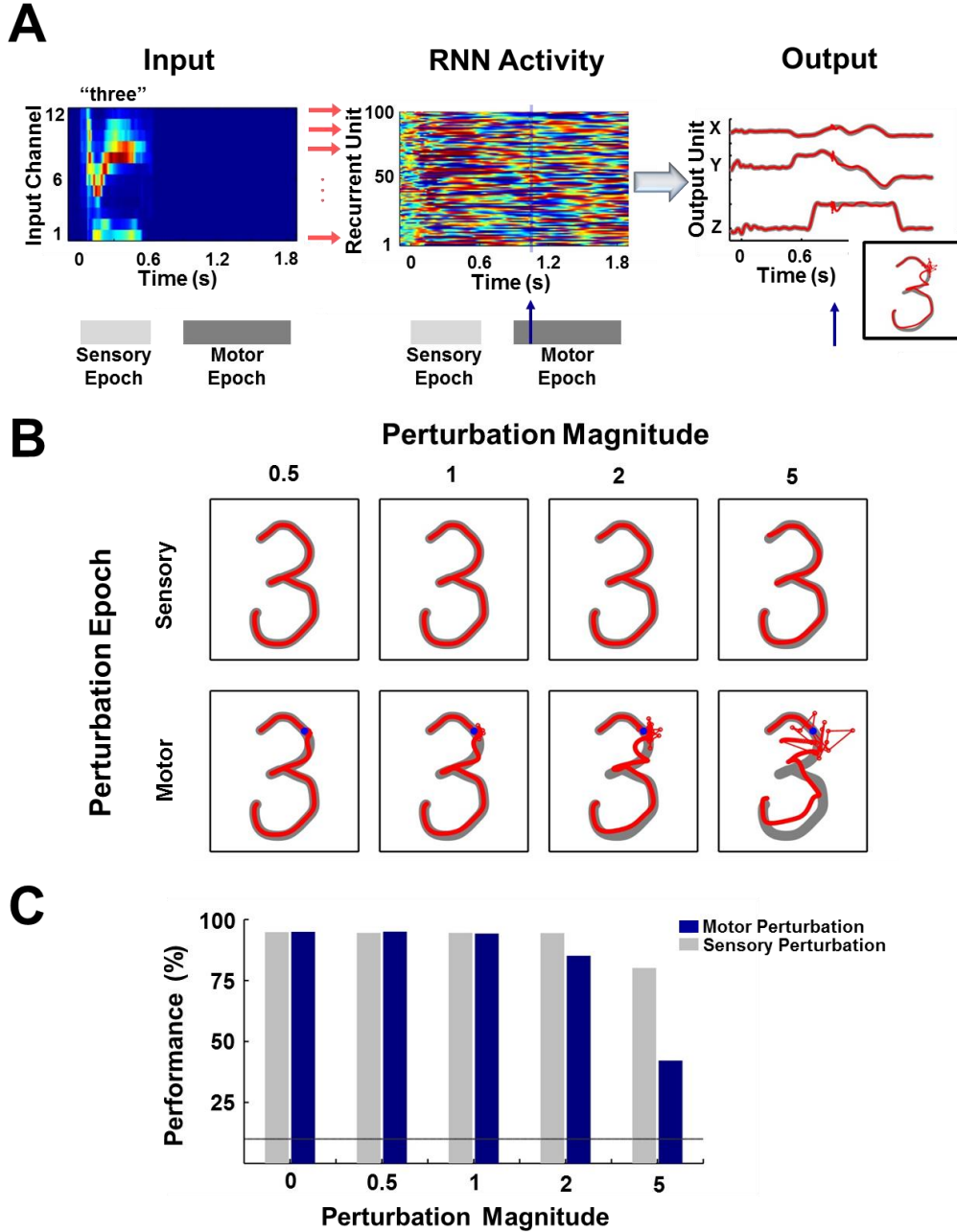


Figure 2: Digit transcription is robust to perturbations during the sensory and motor epochs.

(A) Schematic of a perturbation experiment. The motor trajectory of a trained RNN ($N=2100$; 100 sample units shown) for the spoken digit “three”, is perturbed with a 25 ms pulse (amplitude = 2). The pulse (blue arrow) causes a disruption of the network trajectory, but the trajectory quickly recovers and returns to the dynamic attractor, as is evident from the plots on the right comparing the output unit values and the transcribed pattern for a trial with (red forefront) and without (gray backdrop) the perturbation. **(B)** Sample motor patterns generated by the network in response to perturbations of increasing magnitude, applied either during the sensory or motor epochs. Sensory epoch perturbations were applied halfway into the epoch,

while motor epoch perturbations were applied at the 10% mark of the epoch (indicated by a blue dot). **(C)** Impact of perturbations on transcription performance (measured by the deep CNN classifier) for test utterances. Bars represent mean performance over ten trials, with a different (randomly selected) perturbation pulse applied at each trial. Line indicates chance performance. The performance measures establish that the encoding trajectories are stable to noise perturbations, with transcription performance degrading gracefully as the perturbation magnitude increases. Furthermore, at all perturbation magnitudes, the sensory encodings are more robust than their motor counterparts due to the suppressive effects of the sensory input. The network was trained on 30 utterances (3 utterances of each digit by 1 subject) and tested on 70 (7 utterances of each digit by 1 subject). I_0 was set to 0.25 during network training, to 0.01 during output training, and to 0 during testing except for the duration of the perturbation pulse.

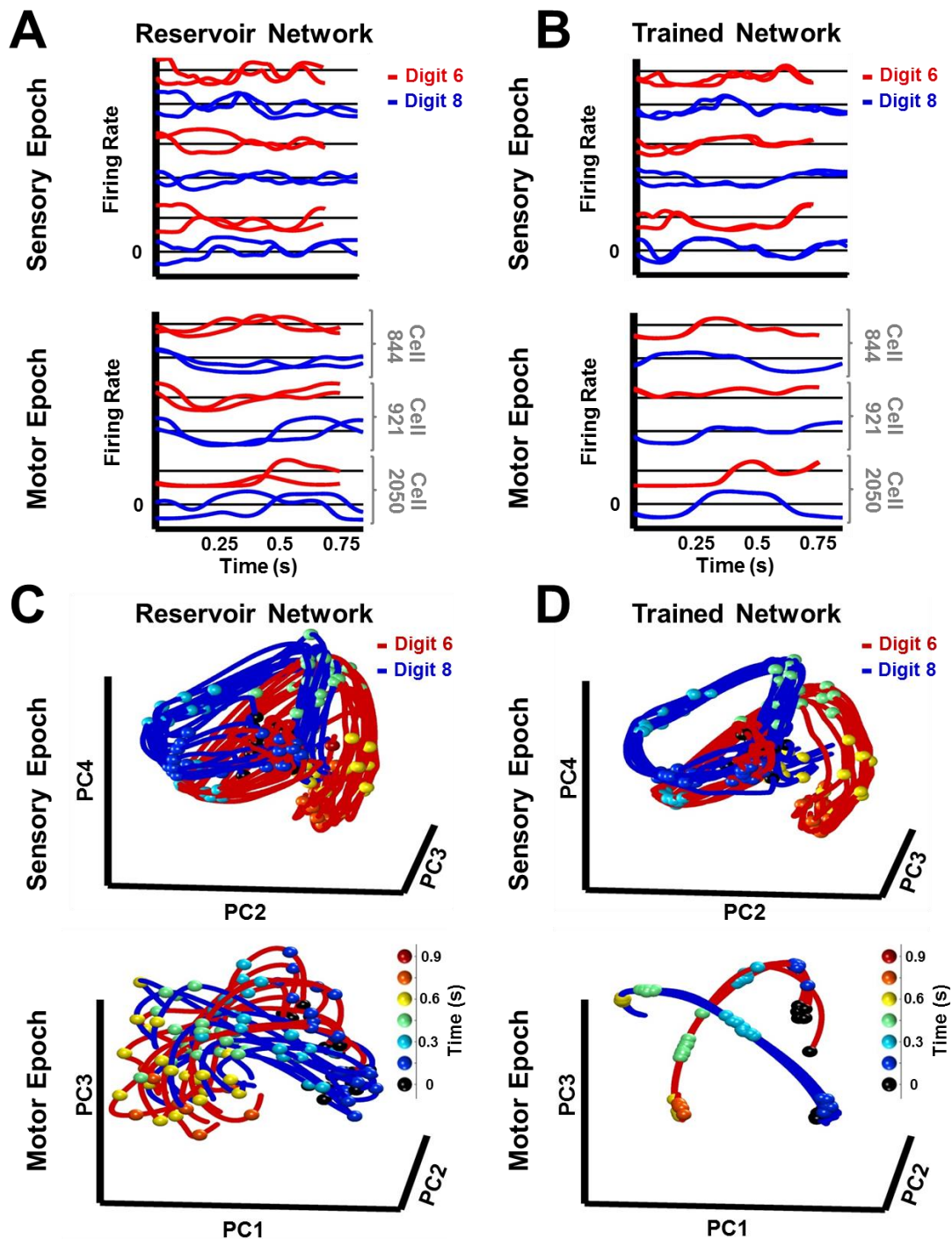


Figure 3: Trained RNNs generate convergent continuous neural trajectories in response to different instances of the same spatiotemporal object.

(A-B) Neural activity patterns of three sample units of a reservoir (A) and trained (B) network, in response to a trained and a novel utterance each of the digits “six” (red traces) and “eight” (blue traces) during the sensory (top) and motor (bottom) epochs. Utterances of similar

duration were chosen for each digit, to allow for a direct comparison, without temporal warping, of the corresponding pair of sensory epoch traces. **(C-D)** Projections in PCA space of the sensory and motor trajectories for 10 utterances each of the digits “six” and “eight” generated by the reservoir **(C)** and trained **(D)** networks. Colored spheres represent time intervals of 150 ms. Compared to the reservoir network, in the trained RNN the activity patterns in response to different utterances of the same digit are closer, and the trajectories in response to different digits are better separated. Both networks were composed of 2100 units. Network training was performed with 30 utterances (1 subject, 10 digits, 3 utterances per digit). l_0 was set to 0.5 during network training, and to 0 while recording trajectories for the analysis.

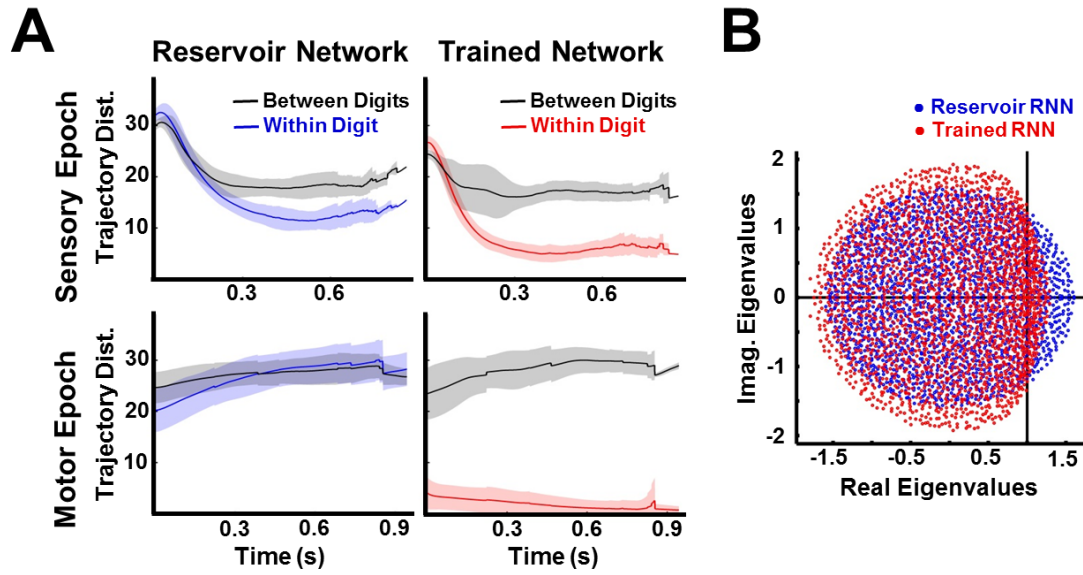


Figure 4: Trained RNNs encode both sensory and motor objects as well separated neural trajectories.

(A) Euclidean distance between trajectories of the same digit (within-digit) versus those of different digits (between-digit). At each time step, the trajectory distances represent the mean and SD (shading) over pairs of one hundred utterances (1 subject, 10 digits, 10 utterances per digit). During the sensory epoch, training brings trajectories for the same digit closer together, while maintaining a large separation between trajectories of different digits, thereby improving discriminability. A similar, but stronger, effect is observed during the motor epoch. **(B)** Comparison of the eigenspectrum of the recurrent weight matrix (W^R) in a reservoir and trained network. Both networks were composed of 2100 units. Network training was performed with 30 utterances (1 subject, 10 digits, 3 utterances per digit). l_0 was set to 0.5 during network training, and to 0 while recording trajectories for the analysis.

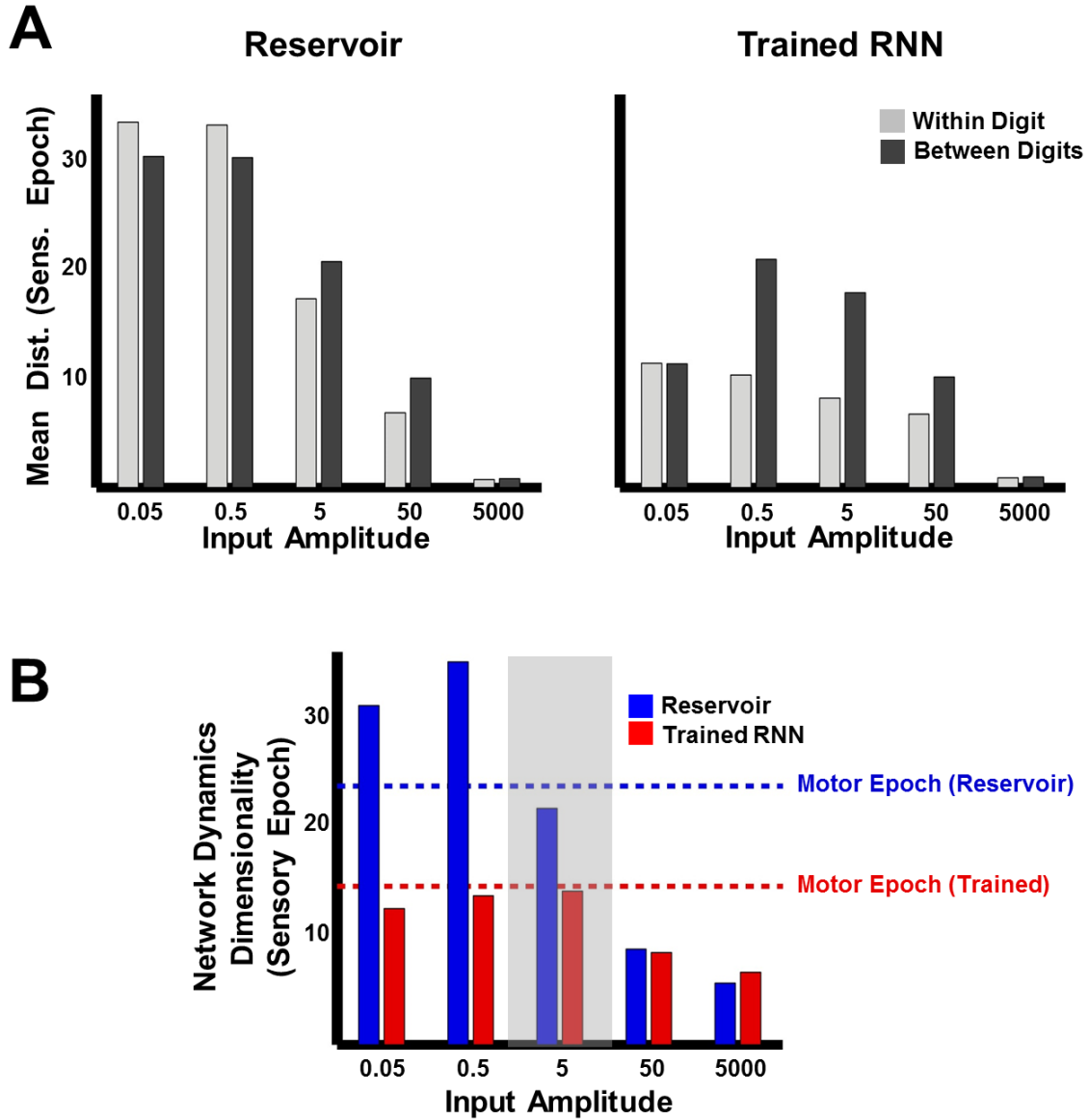


Figure 5: Trajectory separation in reservoir and trained RNNs as a function of input amplitude.

(A) Comparison of mean within- and between-digit distances of the sensory epoch trajectories in reservoir and trained networks ($N=2100$) at different input amplitudes. Bars represent mean of the time-averaged distances for all utterances of all digits (1 subject, 10 digits, 10 utterances per digit). **(B)** Dimensionality of sensory epoch trajectories in the reservoir and trained networks at different input amplitudes. Simulations, including training, in all other figures were performed at an input amplitude of 5 (gray highlight). Dashed lines indicate the dimensionality of the motor epoch trajectories in the reservoir (blue) and trained (red) networks, when the input amplitude was 5. Network training was performed with l_0 set to 0.25, and trajectories were recorded with l_0 set to 0.

warping of the input. **(B)** Mean time-averaged Euclidean distance between sensory trajectories encoding warped and reference utterances of the 10 digits in each of the three networks, over a range of warp factors. Error bars (not visible) indicate standard errors of the mean over 10 test trials. Gray arrows indicate the warp factors at which the networks were trained. **(C)** Transcription performance (measured by the deep CNN classifier) of the three networks on utterances warped over a range of warp factors. The results corroborate the measurements in (B) and show that a sensorimotor trained RNN is more resistant to temporal warping. All networks were composed of 2100 units. Network training was performed with 30 utterances (1 subject, 10 digits 1 utterance per digit, 3 warps per utterance). l_0 was set to 0.25 during network training, and to 0.05 during output training and testing. Reference trajectories for the distance analysis were recorded with l_0 set to 0.

Supplementary Methods:

Trajectory Distance Decomposition

The analysis in **Supplementary Fig. 3** was performed on trajectory pairs encoding utterance pairs. To account for the difference in trajectory durations during the sensory epoch, each trajectory pair had to be temporally aligned. At each time step along the trajectory encoding one utterance, it was aligned to the closest point along the trajectory encoding the other utterance (dynamic time warping). Euclidean distance calculations and decompositions were then performed for the aligned sequence of time points.

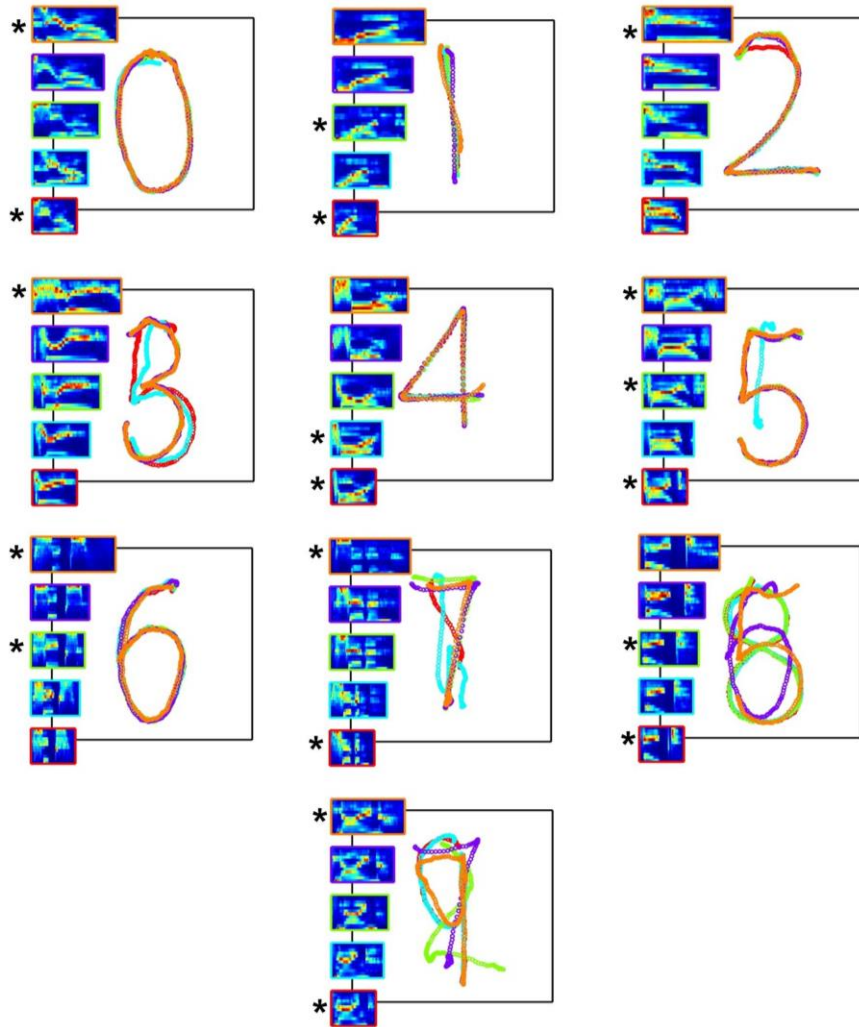
The interaction between the total trajectory deviation and the difference in the recurrent components at time step t (**Supplementary Figs. 2 and 3**), can be expressed in terms of how much the recurrent component difference amplifies the trajectory deviation at time step t . If such an amplification exists at each time step, one can conclude that the two trajectories exponentially diverge from each other. An amplification of the trajectory deviation at t , in the

next time step $t+1$ is indicated by $\frac{\Delta \mathbf{x}_{t+1} \cdot \Delta \mathbf{x}_t}{\|\Delta \mathbf{x}_t\|^2} > 1$. From Equation S2 (**Supplementary Fig. 2**),

$$\begin{aligned} \frac{\Delta \mathbf{x}_{t+1} \cdot \Delta \mathbf{x}_t}{\|\Delta \mathbf{x}_t\|^2} &= \left(\frac{\tau - 1}{\tau} \right) \frac{\Delta \mathbf{x}_t \cdot \Delta \mathbf{x}_t}{\|\Delta \mathbf{x}_t\|^2} + \left(\frac{1}{\tau} \right) \frac{\Delta \mathbf{R}_t \cdot \Delta \mathbf{x}_t}{\|\Delta \mathbf{x}_t\|^2} + \left(\frac{1}{\tau} \right) \frac{\Delta \mathbf{I}_t \cdot \Delta \mathbf{x}_t}{\|\Delta \mathbf{x}_t\|^2} \\ &= \left(\frac{\tau - 1}{\tau} \right) + \left(\frac{1}{\tau} \right) \left(\frac{\Delta \mathbf{R}_t \cdot \Delta \mathbf{x}_t}{\|\Delta \mathbf{x}_t\|^2} + \frac{\Delta \mathbf{I}_t \cdot \Delta \mathbf{x}_t}{\|\Delta \mathbf{x}_t\|^2} \right) \end{aligned} \quad (4)$$

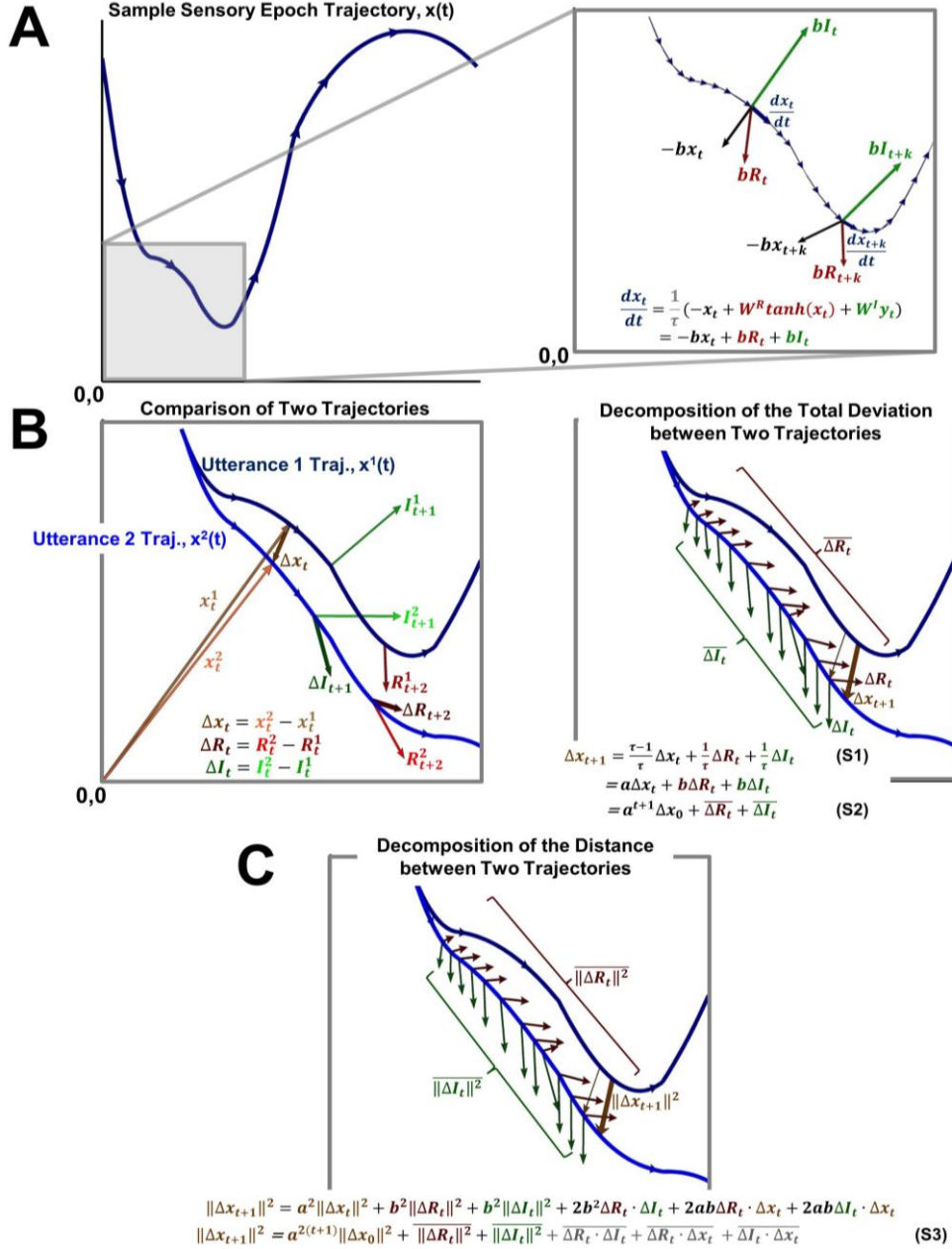
Therefore, $\frac{\Delta \mathbf{x}_{t+1} \cdot \Delta \mathbf{x}_t}{\|\Delta \mathbf{x}_t\|^2} > 1$ if and only if $\left(\frac{\Delta \mathbf{R}_t \cdot \Delta \mathbf{x}_t}{\|\Delta \mathbf{x}_t\|^2} + \frac{\Delta \mathbf{I}_t \cdot \Delta \mathbf{x}_t}{\|\Delta \mathbf{x}_t\|^2} \right) > 1$, which simplifies to $\frac{\Delta \mathbf{R}_t \cdot \Delta \mathbf{x}_t}{\|\Delta \mathbf{x}_t\|^2} > 1$ during the motor epoch.

Supplementary Figures:



Supplementary Figure 1: Transcription performance of an RNN trained only during the motor epoch.

Overlaid outputs of a motor-trained RNN ($N=4000$) for 5 sample utterances of each of the 10 digits used in the spoken-to-handwritten digit transcription task. Transcription performance of the motor-trained RNN is poorer than its sensorimotor trained counterpart (**Fig. 1B**). Each output pattern is color-coded to the bounding box of the corresponding cochleogram (insets). Sample utterances shown are a mix of trained (*) and novel utterances, and are the same ones shown in **Fig. 1B**. The network was trained on 90 utterances (10 digits, 3 subjects, 3 utterances per subject per digit). I_0 was set to 0.5 during network training, and to 0.05 during output training and testing.

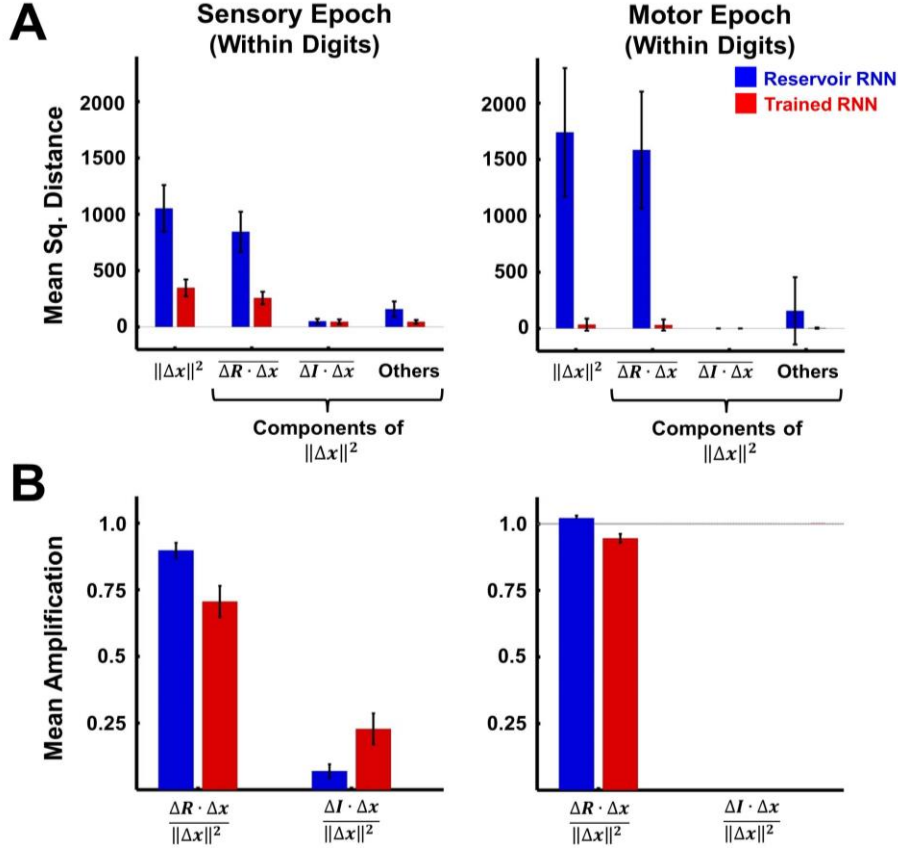


Supplementary Figure 2: Schematic description of the decomposition of trajectories and trajectory distances into recurrent and input components.

(A) Left panel. Schematic of the evolution of a trajectory $x(t)$. Right panel. The evolution of the trajectory in phase space between time steps t and $t+1$ $\left(\frac{dx_t}{dt}\right)$, can be decomposed into three

component vectors: recurrent (red), input (green), and a passive component (black, which always points towards the origin). The sum of these vectors must equal the net movement of the trajectory between those time steps. **(B)** Left panel. The total deviation between two trajectories $x^1(t)$ and $x^2(t)$ at time step $t+1$ (Δx_{t+1}), can be viewed similarly as being composed of the recurrent (ΔR_t), input (ΔI_t) and total (Δx_t) deviations at time t . Right panel. The total deviation at t , in turn, can be decomposed into the recurrent and input deviations at the

previous time steps (i.e. Equation S1 may be viewed as a recurrence relationship). Thus, the total deviation at $t+1$ can be decomposed into recurrent and input deviation histories ($\overline{\Delta R_t}$ and $\overline{\Delta I_t}$, respectively, where the bar represents an the exponentially weighted sum of the history up to time t). The vectors associated with ΔR and ΔI are plotted at different time points solely for visualization purposes. **(C)** The squared Euclidean distance between the two trajectories at time $t+1$ ($\|\Delta x_{t+1}\|^2$) can be similarly decomposed in terms of its recurrent and input components. In addition to the recurrent and input deviation magnitude histories ($\|\overline{\Delta R_t}\|^2$ and $\|\overline{\Delta I_t}\|^2$, respectively), such a decomposition yields several interaction terms (dot products) due to its quadratic nature. Among others, these include the history of interactions between the recurrent and total trajectory deviations ($\overline{\Delta R_t \cdot \Delta x_t}$), and between the input and total trajectory deviations ($\overline{\Delta I_t \cdot \Delta x_t}$). Trajectories must be temporally aligned before their distances are decomposed, because the input and recurrent deviations are most relevant where the trajectories are close to each other in phase space. Here, trajectories are depicted as naturally aligned and in 2D phase space for illustrative purposes only.



Supplementary Figure 3: Trained RNNs coalesce within-digit trajectories by suppressing trajectory deviations.

(A) Decomposition of the squared Euclidean distance ($\|\Delta x_{t+1}\|^2$) between within-digit trajectories (sensory epoch, left panel; motor epoch, right panel) in a trained versus reservoir network ($N=2100$). Bars represent the mean of the time-averaged distances between all pairs of novel and trained utterances for each digit, and error bars indicate the SD. The decomposition reveals that, in both networks, the single largest contribution to the squared Euclidean distance comes from the interaction between the recurrent and total trajectory deviations ($\Delta R \cdot \Delta x$). **(B)** Amplification of the total within-digit trajectory deviations (Δx_t) by the recurrent (ΔR_t) and input (ΔI_t) deviations in the reservoir and trained networks (sensory epoch, left panel; motor epoch, right panel). Taken together, these quantities represent the total amplification of the trajectory deviation at time step t in the next time step $t+1$ (see Supplementary Methods), and draw relevance from the fact that they represent the most important interaction terms in (A). Bars represent the mean of the time-averaged amplification factors between all pairs of novel and trained utterances for each digit, and error bars indicate the SD. During the sensory epoch, recurrent amplification of the trajectory deviation is greatly reduced after training, indicating a realignment of the recurrent drive in the two trajectories along the same direction. The input driven amplification of the trajectory deviation observes an increase after training, a consequence of the reduced separation between trajectories (i.e. the denominator, $\|\Delta x\|^2$, in Equation 4). During the motor epoch, the recurrent deviation is solely responsible for amplifying/suppressing the trajectory deviation. Training decreases the

amplification factor from an average value that is greater than 1 (recurrent amplification of trajectory deviations) to one that is less than 1 (recurrent suppression of trajectory deviations), resulting in a dynamic attractor. Network training was performed on 30 utterances (1 subject, 10 digits, 3 utterances per digit) with I_0 set to 0.25. The set of novel utterances was comprised of 70 utterances (1 subject, 10 digits, 7 utterances per digit), and trajectories were recorded with I_0 set to 0.